BIOCHEMISTRY
including biophysical chemistry & molecular biology

ARTICLE

pubs.acs.org/biochemistry

Making Ends Meet: The Importance of the N- and C-Termini for the Structure, Stability, and Function of the Third SH3 Domain of CIN85

D. Philippe,[†] A. Ababou,[‡] X. Yang,[†] R. Ghosh,[§] T. Daviter,[∥] J. E. Ladbury,[§,⊥] and M. Pfuhl*[,†,@]

[†]Department of Biochemistry, University of Leicester, Lancaster Road, Leicester LE1 9HN, U.K.

[‡]Department of Chemical and Biological Sciences, University of Huddersfield, Queensgate, Huddersfield HD1 3DH, U.K.

[§]Department of Structural and Molecular Biology, University College London, Gower Street, London WC1E 6BT, U.K.

[∥]ISMB Biophysics Centre, Department of Biological Sciences, Birkbeck, University of London, Malet Street, London WC1E 7HX, U.K.

[⊥]Department of Biochemistry and Molecular Biology and Center for Biomolecular Structure and Function, University of Texas M. D. Anderson Cancer Center, 1515 Holcombe Boulevard, Houston, Texas 77005, United States

Supporting Information

ABSTRACT: SH3 domains are common structure, interaction, and regulation modules found in more than 200 human proteins. In this report, we studied the third SH3 domain from the human CIN85 adaptor protein, which plays an important role in both receptor tyrosine kinase downregulation and phosphatidylinositol 3 kinase inhibition. The structure of this domain includes an additional 90° kink after the last canonical β-strand and features unusual interactions between the termini well outside the boundaries of the standard SH3 domain definition. The extended portions of the domain are well-structured and held together entirely by side chain−side chain interactions. Extensive expression screening showed that these additional contacts provide significantly increased stability to the domain. A similar 90° kink is found in only one other SH3 domain structure, while side chain contacts linking the termini have never been described before. As a result of the increased size of CIN85 SH3 domain C, the proximal proline rich region is positioned such that a possible intramolecular interaction is structurally inhibited. Using the key interactions of the termini as the basis for sequence analysis allowed the identification of several SH3 domains with flanking sequences that could adopt similar structures. This work illustrates the importance of careful experimental analysis of domain boundaries even for a well-characterized fold such as the SH3 domain.

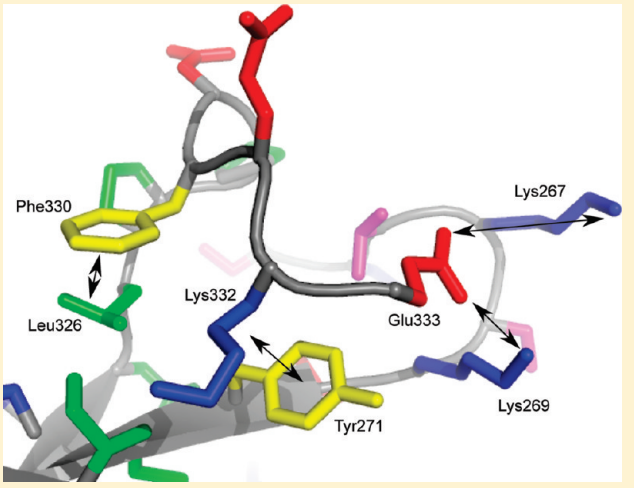

The ability to combine multiple structurally and functionally distinct modules within the same protein has made a significant contribution to the rapid evolution of eukaryotes.[1−4] It also facilitates their investigation by providing ready-made, defined fragments that allow the precise analysis of their structure and function using a divide and conquer approach. Knowledge of the exact domain boundaries is fundamental to obtaining a stable protein fragment that can be used to generate meaningful results.[5] It is well established that a domain that is out of phase by a very small number of residues can lead to unfolded or severely destabilized protein.[6,7] In the case of domains of unknown structure, even the best sequence alignment will leave some uncertainty regarding the first and last residues required for a well-defined, stable, and functional structure, but even when ample structural information is available for a type of domain, it is not necessarily guaranteed that the standard boundaries will be useful for each member of such a family. Such a problem arose in the study of the SH3 domains of the mammalian adapter protein CIN85 (also known as Ruk and CD2AP).

CIN85 is a multifunction adapter or scaffolding protein consisting of three SH3 domains in the N-terminal half of the protein connected by unstructured linkers followed by a proline rich region, a serine rich region, and a coiled coil domain at the C-terminus[8] (Figure 1A). It is best known as a component of the downregulation mechanism of receptor tyrosine kinases in endocytosis.[9] CIN85 is involved in forming a complex of receptors and proteins targeting them for either direct recycling or destruction in the proteasome.[10] The latter requires the formation of a complex with the ubiquitin ligase Cbl via the interaction of the SH3 domains of CIN85 with proline rich motifs at the C-terminus of

Received: December 9, 2010
Revised: March 25, 2011
Published: March 29, 2011

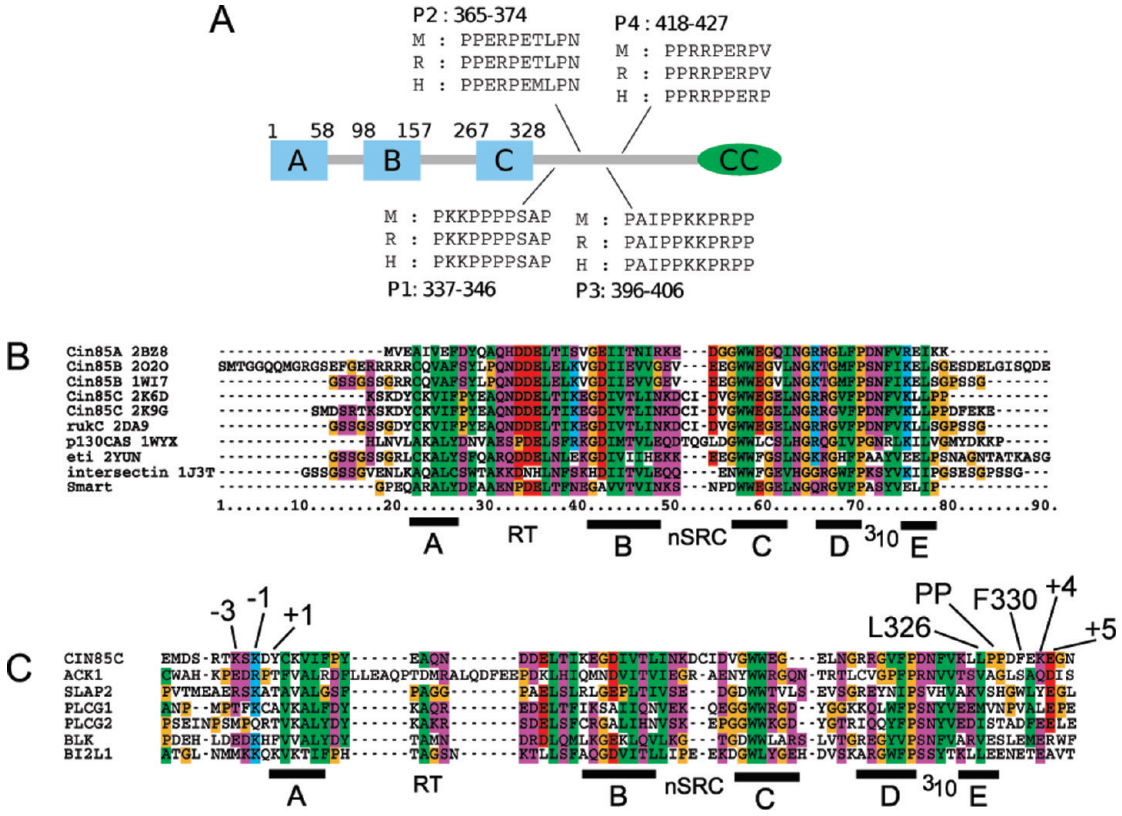

Figure 1. Layout of human CIN85. (A) The three SH3 domains are shown as blue boxes; the coiled coil region is shown as a green ellipse, and the locations of the four proline rich segments following domain C with the actual sequence for human (H), rat (R), and mouse (M) homologues are shown. All residue numbering is shown for the human form of CIN85. Domains and motifs are not drawn to scale. (B) Alignment of the constructs analyzed in this work against the smart profile of the SH3 domain. Colors for conserved residues in both alignments are green for hydrophobic, red for negatively charged, blue for positively charged, magenta for polar, and yellow for glycine or proline. The secondary structure is shown for both alignments with the β-strands depicted as black rectangles and the corresponding identifier from A to E. The loops are shown with their names. The RT loop draws its name from a conserved pair of arginine-threonine residues in the SH3 domain of Src. The n-Src loop draws its name from the SH3 domain of the protein neuronal Src because it has a specific insertion in this loop. The final loop between strands D and E contains a 3_{10}-helix. Sequence alignments are colored for conservation levels of >65%, the exceptions being glycine and proline, which are always colored, provided that more than 50% of the sequences in the alignment have a residue at a given position. (C) Sequence alignment of CIN85 SH3 domain C against all hits of the pattern search. The key charged and hydrophobic residues for the contacts between the N- and C-termini are labeled as described in Materials and Methods. Conserved residues are colored as in panel B.

Cbl.[11] A more direct effect on the regulation of kinase activity was demonstrated for the rat homologue of CIN85, Ruk, when it was shown that it acts as a direct inhibitor of phosphatidylinositol 3-kinase[12] via an interaction with the p85 regulatory subunit for which the SH3 domains are required.[13]

To improve our understanding of the complex interactions required for the diverse biological functions of CIN85 better, we set out to determine the structures of its SH3 domains and investigate their interactions in solution. We characterized SH3 domains A and B in detail using NMR spectroscopy, ITC, and molecular modeling.[14,15] New optimized constructs were generated for the study of larger, multidomain fragments. Unexpectedly, the optimal construct for domain C is significantly longer than the conserved SH3 core. In the three-dimensional (3D) structure, the N- and C-termini extend significantly beyond the customary terminal β-strands, held together by unusual side chain contacts. A sequence search based on the key residues for this interaction in all human SH3 domain sequences identified several that would be predicted to adopt a similar structure, suggesting that our findings are not limited to CIN85 but are of general relevance.

MATERIALS AND METHODS

Sequence Analysis. For the initial design of optimized expression constructs for SH3 domains B and C of CIN85 (Uniprot entry Q96B97), sequences were extracted from Protein Data Bank (PDB) entries for structures of domain B of human CIN85 (2O2O) and rat Ruk (1WI7) as shown in Figure 1B. A comparison of the sequences and structures of domain B with known SH3 domains (see Figure 1B) was used to define the core size for both domains B and C in human CIN85. For the systematic screen, these core domains were extended systematically N- and C-terminally (Figure 2A) by up to 10 amino acids.

A search for potentially similar N- and C-terminal contacts was performed on a sample of all SH3 domains found in the human genome using the Prosite profile PS50002.[16] A total of 267 SH3 domains were found in 203 proteins. Sequences of all SH3 domains were extracted with an additional 20 residues added to the standard Prosite definition (PS50002) at either end.[16] A pairwise comparison was then performed for each domain against the extended sequence of CIN85 domain C (construct 35) to look for the crucial polar and hydrophobic interactions of Lys267 and Lys269 (N − 3 and N − 1)

dx.doi.org/10.1021/bi1019644 |*Biochemistry* 2011, 50, 3649–3659

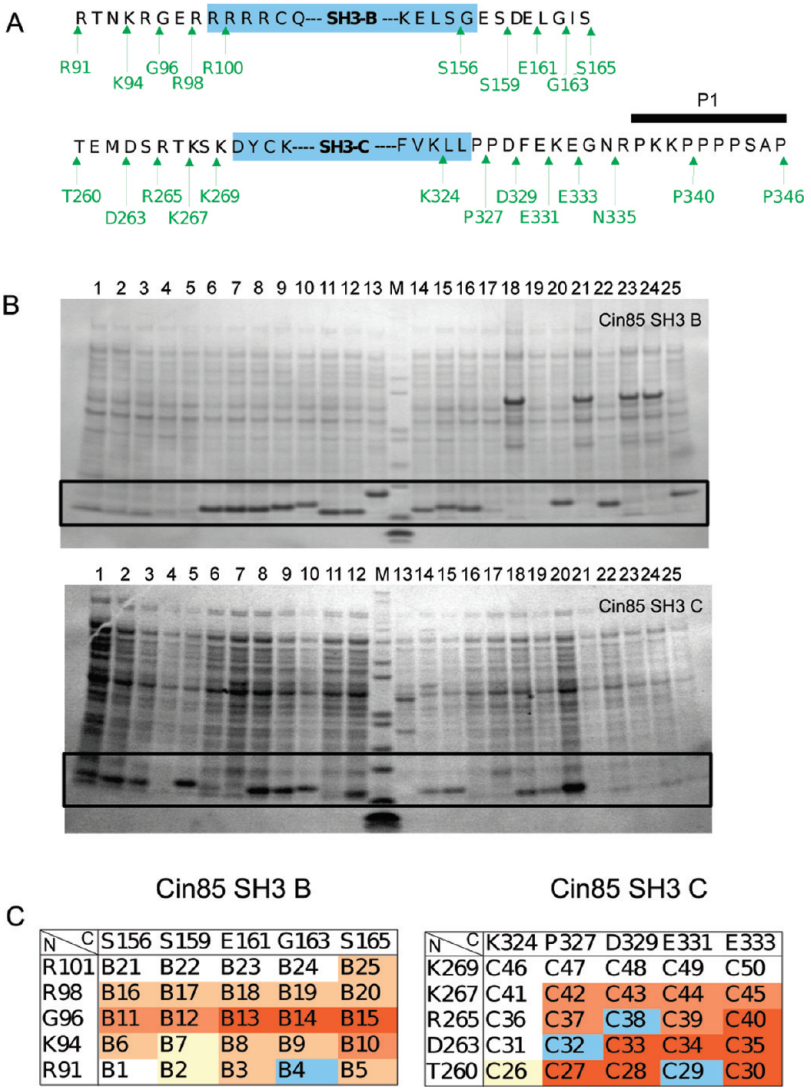

Figure 2. Constructs of CIN85 SH3 domain B and C and their expression. (A) Overview of constructs. Rationally designed constructs based on the CIN85 SH3 domain B solution structure (PDB entry 2O2O) are highlighted in blue. An array of new constructs was created encompassing the extensions colored green (residues shown included). Additional C-termini for constructs C51 (Asn335), C52 (Pro340), and C53 (Pro348), all starting at residue Asp263, not part of the original 5 × 5 screening matrix and used in the study of potential interactions of the P1 segment, are shown for the sake of completeness. As a result, they are not included in panel C. The position of the proline rich motif P1 is indicated above the sequence. (B) Example for expression trials of constructs for domains B (top) and C (bottom) monitored by SDS−PAGE. Samples loaded are the soluble fraction of constructs for the top and bottom panels: lanes 1−5, B21−B25, respectively; lanes 6−10, B16−B20, respectively; lanes 11−15, B11−B15, respectively; lanes 16−20, B6−B10, respectively; and lanes 21−25, B1−B5, respectively(left to right for the top panel); lanes 1−5, C26−C30, respectively; lanes 6−10, C31−C35, respectively; lanes 11−15, C36−C40, respectively; lanes 16−20, C41−C45, respectively; and lanes 21−25, C46−C50, respectively (left to right for the bottom panel). Construct numbers are the same as shown in panel C. The molecular weight marker (mark12, Invitrogen) is in the center lane for both domains and the expected molecular weight for the domains is indicated by a frame. (C) Corresponding construct reference number and soluble protein yield (red > pink > yellow > white) as estimated from SDS−PAGE of the cell lysis supernatant shown in Figure 4B and normalized using other bands in the same lane. Blue color indicates constructs that failed to be cloned.

with Glu333 (C + 5) and Tyr271 (N + 1) with Lys332 (C + 4). The following residues are allowed in the various positions: N − 1 and N − 3, KR; N + 1, FWYALVMTEQKR; C + 4, KRLMIVFWYT; C + 5, DE. In positions N + 1 and C + 4, charged residues are allowed only if they are complementary. To be considered a hit, a sequence has to match all five residues with the allowance of no more than two being shifted by at most one position. The resulting hits were further analyzed by sequence alignment in clustalw[17] against construct C35 using default parameters and displayed in clustalx.[18]

Cloning and Protein Expression. The N/C variations were cloned using the In-Fusion method (Clontech) into in-house bacterial expression plasmid pLEICS-03 that provides an N-terminal His tag with a TEV cleavage site. For protein expression, constructs were transformed into BL21* cells (Invitrogen). Cells were grown at 37 °C, and expression was induced with 0.5 mM IPTG (Melford Laboratories.) at an OD of 0.8 for 4 h. Harvested cells were resuspended in wash buffer [20 mM PO_4 (pH 7.5), 500 mM NaCl, 1 mM β-mercaptoethanol, and 0.02% NaN_3] and opened using an NP40-based lysis solution. The entire screen was conducted in 96-well plates (1 mL/well). For structure determination, proteins were expressed and purified on Fast Flow 6 nickel chelating columns (GE Healthcare) as described previously.[14,19]

dx.doi.org/10.1021/bi1019644 |*Biochemistry* 2011, 50, 3649–3659

CD Spectroscopy. CD data were recorded on a Jasco J700 spectropolarimeter fitted with a Peltier temperature control system. Initial spectra were recorded in rectangular quartz cuvettes (Starna) with a 0.1 mm path length to select a wavelength to monitor thermal unfolding experiments. Thermal unfolding curves were measured for selected constructs of domain C at protein concentrations of 50 μM in standard measurement buffer [20 mM sodium phosphate, 50 mM sodium chloride, 1 mM DTT, and 0.02% sodium azide (pH 7.0)] using a 1 mm path length cuvette at a wavelength of 215 nm using a temperature gradient of 1 °C/min from 5 to 90 °C. Data were recorded at one point per 1 °C. At each point, the CD signal was averaged for 1 s. The unfolding curve was fitted to a two-state unfolding equation in a home-written Mathematica macro that optimized the melting temperature and the slope at unfolding while the initial and final slopes of the curve were optimized manually.

NMR Spectroscopy. NMR spectra for assignment and structure calculation were recorded on 500, 600, and 800 MHz Bruker Avance spectrometers. Sample concentrations ranged from 100 μM for controls and screening of constructs to 0.8 mM for collection of distance constraints. All samples were measured in standard measurement buffer. Standard triple-resonance experiments[20] for backbone and side chain assignment were based on those provided by the manufacturer but extensively modified to improve hardware protection. All experiments for assignment, dynamics, and structure calculation were conducted at 298 K. All spectra analysis, assignment, and extraction of data for further analysis were performed with CCPN analysis.[21] The Lipari−Szabo analysis[22,23] of ^{15}N T_1 and T_2 and heteronuclear NOE data[24,25] was performed using home-written macros in Mathematica.

Structure Determination. The structure calculation was initially based on NOESY cross-peaks collected with a mixing time of 100 ms for ^{15}N-resolved 3D NOESY (860), aliphatic ^{13}C-resolved 3D NOESY (1320), and aromatic ^{13}C-resolved 3D NOESY (72) spectra. All these 2252 peaks were converted into unassigned distance constraints and used directly in CYANA 2.1[26] together with 108 dihedral (Φ and Ψ) constraints extracted from chemical shifts using TALOS.[27] After seven cycles of structure calculation, a total of 2246 peaks were assigned, including the unambiguous identification of the stereochemistry of 24 prochiral groups. The structure was then regularized using REDAC and refined using 62 ^{1}H−^{15}N residual dipolar couplings collected with 10 mg/mL pf1 phage using XPLOR.[28]

Structure Analysis and Comparison. Similar SH3 domains were identified with DALI.[29,30] From the top 300 hits (Z score level of 8.5) of the DALI search, SH3 domains with 69 or more residues were selected for detailed comparison provided that the N- and C-termini were close to each other. There are numerous structures of SH3 domains in the PDB that have N- and C-termini artificially extended by cloning artifacts. To avoid a bias toward these unnatural versions, only a small number of these were selected. All other structures chosen fulfill the selection criteria with their natural sequence. Selected structures were then superposed with DALIlite[29,30] and analyzed with PyMol (http://www.pymol.org).

Molecular Dynamics Simulations. The structure of construct C35 of CIN85C (residues 263−333) used in the MD simulations was taken from our deposited PDB entry 2K9G. Construct C34 lacking residues K332 and E333 was created via removal of those residues. The MD simulation of the fully immersed construct structure in a rectangular box (65.4 Å × 52.2 Å × 60.2 Å) filled with TIP3P water was performed using the Amber program.[31] The simulated C35 and C34 systems consist of 73 and 71 residues, six Na^+ ions, and 4822 and 4840 water molecules, respectively. The time step was 1.5 fs with all bonds fixed to their equilibrium values by SHAKE. The formal charge of the protein of −6 was neutralized via addition of Na^+ ions. The temperature was 300 K. van der Waals interactions were truncated at 10.0 Å, while electrostatic interactions were fully calculated with the particle mesh Ewald method. A solvent equilibration of 25 ps at 300 K was calculated after including the Na^+ ions. Following equilibration, a trajectory of 10 ns was calculated for each construct. The hydrogen bond analysis is based on a distance cutoff of 2.4 Å between the donor and the acceptor (i.e., hydrogen and oxygen or nitrogen) and an angle cutoff between 120° and 180° at the hydrogen atom.

Analytical Ultracentrifugation. The sedimentation velocity experiments were performed at 20 °C on a Beckman XL-I instrument (Beckman Scientific, Palo Alto, CA), equipped with an eight-hole An50-Ti rotor. Sedimentation velocity data for C35 and C53 were acquired in 20 mM phosphate buffer (pH 7.4) with 100 mM NaCl and 1 mM DTT over 16 h at a rotor speed of 42000 rpm in two-channel centerpieces. The proteins were studied over a range of concentrations between 0.07 and 0.4 mg/mL. The data were collected using interference optics and were analyzed with SEDFIT[32] using the $c(s)$ model for the calculation of sedimentation coefficient distributions in which the frictional ratio, bottom of the cell, meniscus, and baseline were floated for the fits. Buffer density (ρ) and viscosity (η) as well as protein partial specific volume (ν_{bar}) used in the analysis were calculated using SEDNTERP version 1.09.[33] The molecular weight estimates of the proteins were calculated in Sedfit from the obtained sedimentation coefficients and frictional ratios.

RESULTS

Cloning and Expression of Domains B and C. Initially, constructs of each of the CIN85 SH3 domains were designed on the basis of the existing solution structure of CIN85 SH3 domain B [PDB entry 2O2O (see Figure 1B)].[15] This structure reveals a rigid domain between R101 and L155. To improve the behavior of new constructs for further studies, we removed the unstructured residues at the N- and C-termini outside the defined region in the new constructs. The analysis of the structure of domain B, together with sequence alignments, was also used to create optimal domain boundaries for the cloning of domain C. Interestingly, the resulting constructs for both domains exhibited limited solubility. To investigate the problem further, a series of constructs was produced for both, by generating an array of five N-termini against five C-termini (Figure 2A) so that 25 constructs were generated and tested for each domain.

To simplify the screening of a significant number of constructs, a high-throughput cloning approach was chosen on the basis of the ligation-independent cloning (LIC) method[34] using the In-Fusion (Clontech) kit that allowed the generation of the constructs and trial expressions in standard multiwell plates.

The results of the expression screen of all constructs of domains B and C were analyzed using sodium dodecyl sulfate−polyacrylamide gel electrophoresis (SDS−PAGE) (Figure 2B) and are summarized in a semiquantitative manner in Figure 2C. Interestingly, both domains required extra residues beyond the optimal boundaries as defined by the structure of domain B. In this domain, there was no correlation in terms of soluble expression between the N- and C-termini. A vague preference for the extension of the C-terminus up to Ser165 is evident, while at the N-terminus, the domain is best behaved when it starts with Gly96. In strong contrast, there is a significant correlation

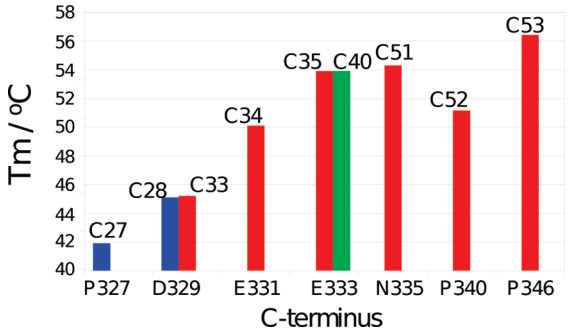

Figure 3. Circular dichroism investigation of the thermal stability of selected constructs. Plot of the fitted melting temperature vs the C-terminal residue of the constructs (residues included). Constructs with different N-termini are shown in different colors: blue for Thr260, red for Asp263, and green for Arg265.

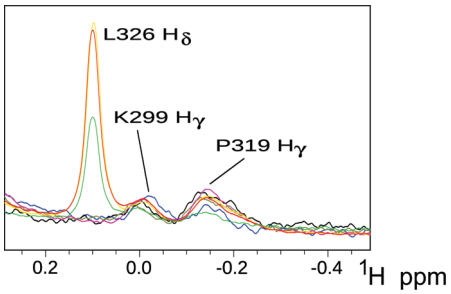

Figure 4. Expanded high-field region of 1D NMR spectra of constructs of domain C: yellow and green for C35 at 1.7 and 0.9 mM, respectively, red for C40, purple for C34, olive for C33, black for C28, and blue for C27. SH3 domain C constructs with C-termini extending to E333 display a peak at ~0.1 ppm corresponding to the Hδ resonances of L326 that is not observed in the shorter constructs.

between the effects of N- and C-terminal extensions of domain C on solubility. It is very clear that neither extension of N- or C-terminus alone achieves much without the other, suggesting the possibility of an important interaction of the termini. Generally, in SH3 domains, the N- and C-termini form an antiparallel β-strand. However, that is well within the defined boundaries. The interactions suggested by this expression screen for domain C are thus much farther outside the usual boundaries of an SH3 domain, suggesting the existence of additional interactions.

Thermal Stability of Versions of Domain C. To explore the properties of the N- and C-terminal extensions in more detail, we performed thermal unfolding experiments for selected constructs. Individual protein domains were purified, and their respective melting temperatures were determined by CD spectroscopy (Figure 3).

The melting temperature increased steeply (by more than 10 °C) from the shortest construct (C27) with its C-terminus at residue Pro327 compared to construct C35 that ends at Glu333 (Figure S1 of the Supporting Information). Further extension of the C-terminus into the proline rich region (Figures 1A and 2A) directly following SH3 domain C did not increase the melting temperature by any significant margin (<2 °C for 13 amino acids added). Only comparatively small effects could be observed for variations at the N-terminus (Figure 3).

Domain C Boundaries and Their Structural Importance. To obtain a more detailed view of the effects of changing the domain boundaries of domain C, one-dimensional (1D) NMR spectra of selected constructs were recorded (Figure 4). While the variations of the melting temperature are significant for some constructs, the changes in the high-field region of the 1D NMR spectrum are striking. A well-defined, isolated peak at 0.1 ppm, corresponding to one of the δ-methyl groups of Leu326, is observed only in constructs C30 (residues 260−333) and C35 (residues 263−333), regardless of the protein concentration. Independent of the N-terminus, this new resonance does not appear in any of the C-terminally shorter constructs. Such a high-field chemical shift can be produced only in a protein by an aliphatic proton strongly shielded by packing to an aromatic ring. The nearest aromatic residue is Phe330, but both Leu326 and Phe330 are also present in the shorter constructs that do not show the high-field shifted peaks of Leu326. This infers that the shielding of Leu326 requires Lys332 and Glu333 and that at least one, if not both, of these residues must make important contacts.

Structure and Dynamics of Domain C. To understand the variations in stability and the striking differences in the NMR spectra among different domain C constructs better, we determined the solution NMR structure of the construct with high thermal stability, C35 (residues Asp263−Glu333 in full-length CIN85). The domain was assigned to >95%, and the structure was calculated with distance constraints obtained from 3D ^{15}N- and ^{13}C-resolved NOESY spectra, backbone dihedral constraints, and residual dipolar couplings (RDC). The latter were collected to ensure a good structural definition of the extended N- and C-termini for which only few NOESY-based distance constraints were obtained.

The family of structures was in good agreement with an average backbone root-mean-square deviation (rmsd) of 0.47 Å (Figure 5A) and with good stereochemical characteristics as indicated by 89% of all residues being in the favored region of the Ramachandran plot. Standard parameters for the structure calculation are summarized in Table 1. The structure was deposited as PDB entry 2K9G.

The core domain is a typical β-barrel formed by five antiparallel β-strands, with the standard RT and n-Src loops connecting strands A, B, and C [A with B and B with C, respectively (Figure 5B)]. However, while the SH3 domain fold is similar to domain B,[15] this new structure reveals an additional structured region outside the boundaries of a typical SH3 domain. Instead of assuming an undefined conformation after the end of the last β-strand at Lys324, the polypeptide backbone at the C-terminus continues for a short distance in an extended conformation until it folds into a 90° kink between Pro328 and Asp329. Subsequently, it crosses over strand A making hydrophobic contacts between Phe330 and Leu326 and between Lys332 and Tyr271 (Figure 5C). The N-terminus in contrast continues only a short distance crossing under the last stretch of the polypeptide chain so that two positively charged amino acids at the N-terminus (Lys267 and Lys269) are positioned close to the last residue Glu333 (Figure 5D). The side chain of the latter is very close in most structures of the family to the side chains of Lys267 and Lys269. This contact is supported by the existence of a small number of NOEs between these parts of the protein (for details, check the constraint list available from PDB entry 2K9G).

The Lipari−Szabo analysis of the backbone dynamics (Figure 5F) of domain C shows that these residues are still relatively well structured with order parameters of ~0.6. This is in good agreement with the residue specific rmsd values (Figure 5E) that show them to be well below 1.0 Å for Lys332 (0.5 Å) and Glu333 (0.6 Å) as well as Lys267 (0.3 Å) and Lys269 (0.2 Å). This suggests that a hydrophobic contact between

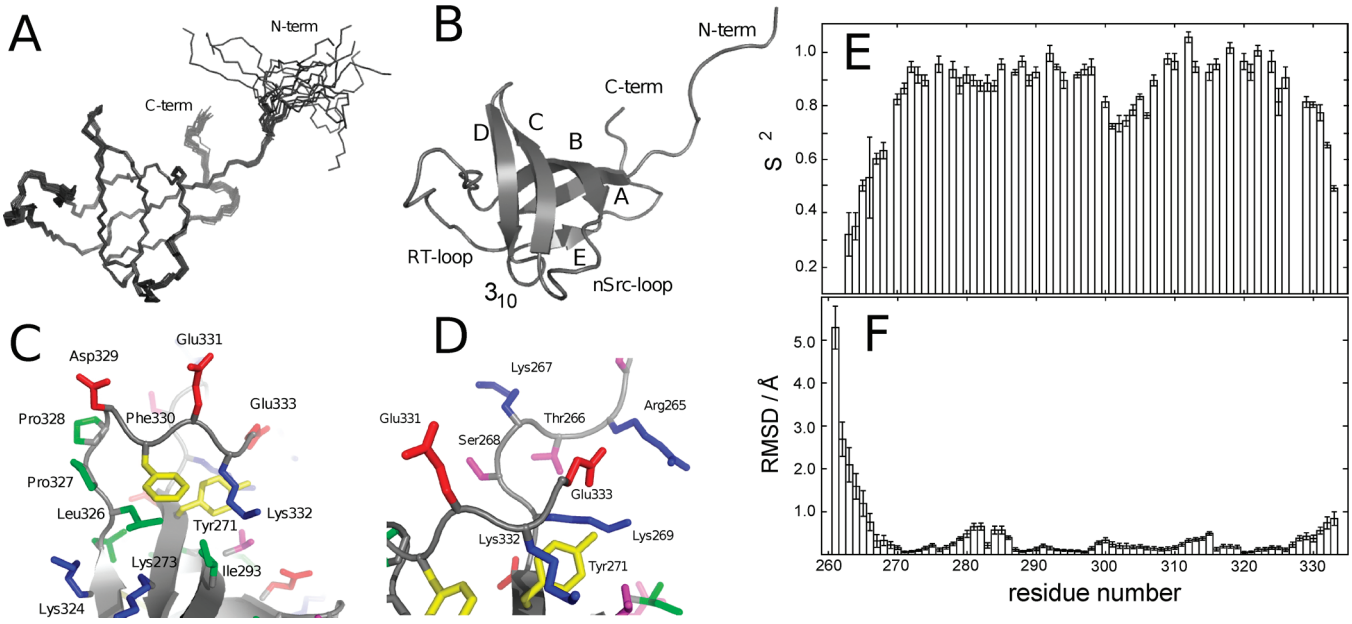

Figure 5. Structure and dynamics of domain C. (A) Wire representation of the top 20 structures from the XPLOR RDC refinement. (B) Secondary structure cartoon, with the same orientation as panel A. (C) Detailed view of the 90° kink around Asp329 and the contact between Phe330 and Leu326. (D) Detailed view of the stabilizing interaction between the N-terminal positively charged Arg265, Lys267, and Lys269 with the C-terminal Glu333 and the hydrophobic contact of Tyr271 and Lys332. (E) NMR order parameters for backbone amide groups. (F) Average backbone rmsd values for the top 20 structures shown in panel A. Fitting errors for the order parameters and standard deviations for the rmsd values are shown as error bars.

Table 1. Structural Statistics for Domain C, Including RDC Refinement[a]

input constraints	
no. of NOE-derived distances	1364
no. of backbone dihedral angle (Φ and Ψ) constraints	108
no. of backbone HN residual dipolar coupling constants	62
structure statistics	
backbone rmsd (Å) (residues D263−E333, N, Cα, C′)	0.47
residues in preferred region of Ramachandran plot (%)	89.0
CING score: residues in green and orange (%)	78.0
average/maximal violation of NOE constraints (Å)	0.02/0.13
average/maximal violation of dihedral constraints (deg)	2.1/12.4
average/maximal violation of RDC constraints (Hz)	0.11/0.57

[a] More details for the structural quality are available from PDB entry 2K9G via the CING link. The CING score refers to the color codes calculated as a summary of different quality assessments for each residue. Residues with green are perfectly OK; residues with orange are not quite perfect but acceptable, and residues with red have a problem. The combination of residues coded in green and orange can be taken to be acceptable, and a higher percentage indicates a better quality of the structure.

Lys332 and Tyr271 as well as a salt bridge between Glu333 and the two positively charged amino acids at the N-terminus may exist, even though the latter might be more dynamic than the former.

Mechanism of Stabilization. NMR spectra suggested that the hydrophobic contact of Leu326 with Phe330 observed in the solution structure is only stable when residues Lys332 and Glu333 are present in the construct (Figure 4). To gain better insight into the relevance of these residues for the stability of the domain, molecular dynamics simulations were performed for constructs C34 (residues 263−331) and C35 (residues 263−333) using our NMR structure of C35 as the starting structure for C35 and C34 (we deleted the last two residues of C35).

Analysis of distances between side chain atoms of Leu326 and the benzene ring of Phe330 over a trajectory of 10 ns clearly shows the presence of the Phe330−Leu326 contact during the entire MD trajectory in construct C35 (Figure 6A). Instead, for C34, this contact lasts up to 7.2 ns and then breaks apart. This can be easily visualized upon comparison of the Leu326−Phe330 cluster at different snapshots of 1, 5, and 10 ns (Figure 6B). At 10 ns, the Phe330 benzene ring rotates and the Leu326 side chain moves away from the benzene ring. In C35, the residues hold their positions very much unchanged for 10 ns. Even before the cluster finally breaks apart for C34, the amplitude of fluctuations in the Leu326−Phe330 distances is substantially larger for C34 than for C35. These observations clearly suggest that the Phe330−Leu326 contact is significantly more stable in C35 than in C34.

The mechanism through which this is achieved is also evident in the simulations. There are polar contacts for Glu331 and Glu333 toward the N-terminus in C35. In C34, the side chain of Glu331 has a very short-lived H-bond to the side chain of Lys269, appearing for only ∼3.5 ns (Figure S2 of the Supporting Information). However, in C35, Glu331 keeps a fairly stable distance with the side chain of Lys269 and could form a hydrogen bond by the end of the trajectory. Glu333 has alternate contacts between its side chain and backbone carboxylate group and the side chain of Lys269. In addition to the C-terminal glutamates, Lys332 also appears to be important by making stable hydrophobic contacts throughout the trajectory between its side chain and the side chain of Tyr271. These contacts are supported by intermittent polar contacts of the amino end group of Lys332 with the side chain of Asp292 and the backbone of Ile293, in good agreement with differences in HSQC spectra of constructs C35 and C33 (Figure S3 of the Supporting Information).

dx.doi.org/10.1021/bi1019644 |*Biochemistry* 2011, 50, 3649–3659

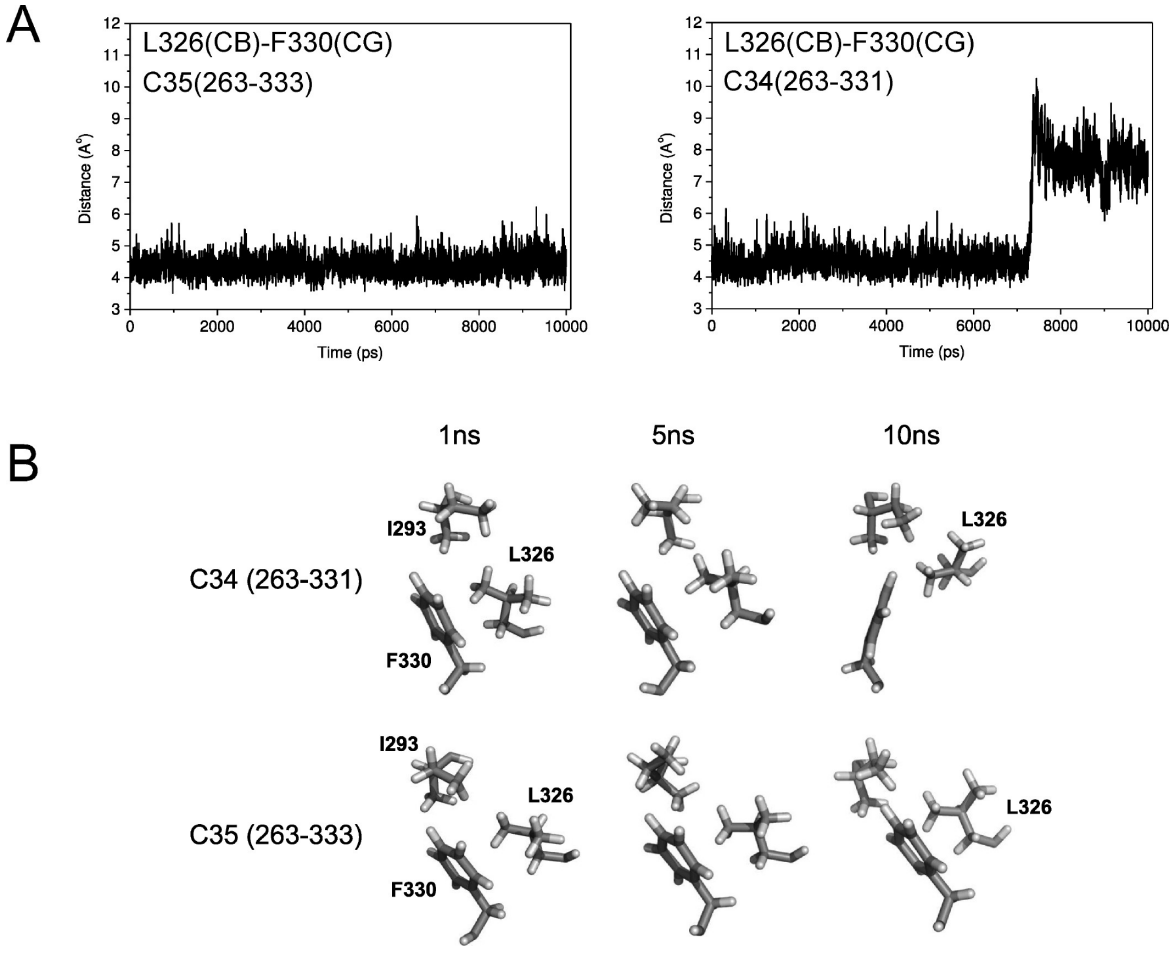

Figure 6. Results of a 10 ns molecular dynamics trajectory of constructs C35 and C34. (A) Time development of key distances involving the N- and C-termini. The distance from Cβ of L326 to Cγ of F330 is shown for both constructs C35 and C34. (B) Structural snapshots of the interaction of L326 with F330 at three time points of the trajectory for the two constructs, C35 and C34.

Structural Comparison with Other SH3 Domains. Recently, the structure of the equivalent SH3 domain C from Ruk was determined in solution.[35] Interestingly, this domain was expressed in a shorter construct, encompassing residues 313−371 in Ruk (corresponding to residues 267−328 in human CIN85). Superposition of the structures in Figure 7 shows that the domains are virtually identical but that the construct from rat CIN85 is shorter and lacks the kinked C-terminus seen in our structure of human CIN85 domain C.

On the basis of the observation of the unusual kinked C-terminus in SH3 domain C of CIN85, a DALI search was performed to determine whether such an unusual structural feature in an SH3 domain had been previously observed. Of the top 300 hits resulting from a DALI search, those with 69 or more residues were selected for analysis. A total of five other domains were identified in this way and superimposed on the structure of domain C (Figure 7). It is noticeable that there were a significant number of SH3 domain structures in the PDB that met the length criterion. However, a large number of them reach only such a length because of artificial extensions very likely due to cloning artifacts. It is worth noting that these extensions are vaguely in the same area as for our domain C but do not make any contacts (Figure 7 and Figure S4 of the Supporting Information).

In stark contrast, the crystal structure of the SH3 domain of p130cas[36] shows a similar kink of the C-terminus just after the last β-strand of the canonical fold followed by a well-defined extended structure. While the extended N- and C-termini of our domain C appear to be held together by side chain contacts, the corresponding extensions in p130cas assume a very different fold by forming a short antiparallel β-sheet (Figure 7 and Figure S4 of the Supporting Information)

Sequence Profile Searches. To determine if similarly extended structures might exist in other SH3 domains, we analyzed the flanking sequences of all SH3 domains found in the human genome to limit the sample size. Using the prosite motif for SH3 domains (PS50002) resulted in the identification of 267 SH3 domains in 203 proteins. In the resulting sequence alignment, the key residues for the salt bridge are found at positions N − 1 and N − 3 (Lys267 and Lys269, respectively) at the N-terminus, and the glutamate residue (Glu333) at the C-terminus is found at position C + 5 beyond the end of the motif. The key residues for the hydrophobic interaction are located at positions N + 1 (Tyr271) and C + 4 (K332). The latter is a polar residue but has a sufficient number of aliphatic CH_2 groups for a hydrophobic contact. A systematic search for conserved residues at these positions produced several hits, shown aligned in Figure 1C. The alignment was then used for a manual search for residues compatible

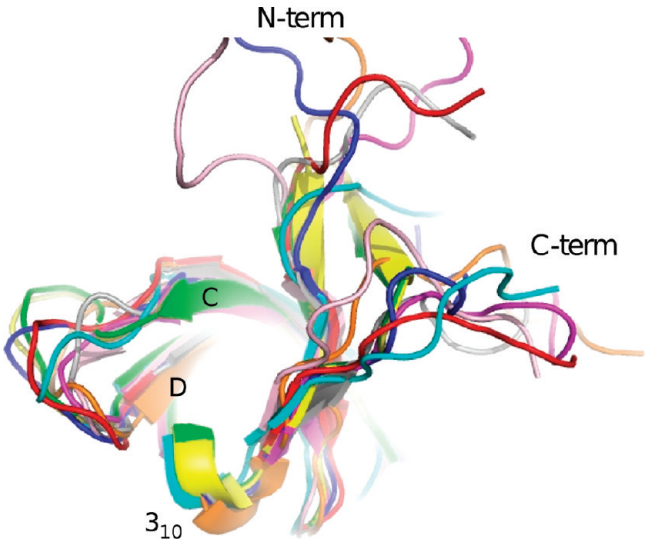

Figure 7. Comparison of the structure of construct C35 of human CIN85 domain C (PDB entry 2K9G) with similar SH3 domains containing extended termini. CIN85 domain C (blue) is superimposed with SH3 domains from rat CIN85 (third domain, red, PDB entry 2DA9), p130CAS (two crystal forms, yellow and green, PDB entry 1WYX), intersectin (purple, PDB entry 1J3T), thyroid receptor interacting protein (cyan, PDB entry 2CT4), growth factor receptor-bound protein (orange, PDB entry 1GBR), Rho GTPase activating protein (pink, PDB entry 2DL8), and ENOS trafficking inducer (gray, PDB entry 2YUN). The structures from PDB entries 2DA9, 2CT4, 2DL8, and 2YUN are artificially extended N- and C-terminally (Figure 1B). Secondary structure elements in the vicinity are labeled.

with a kink close to the double proline in C35 (Pro327 and Pro328) as well as hydrophobic residues like F330 and L326 able to form a contact stabilizing the kink (Figures 5C and 6). The SH3 domain of PLCG1 has a proline shifted by one residue and hydrophobic residues as required. ACK1 lacks both proline as well as suitable hydrophobic residues, while SLAP2 has the required hydrophobic amino acids but lacks a proline. In the other domains, there are no suitable matches for the prolines and the equivalent to position 330 in CIN85 domain C is occupied by charged or hydrophilic residues, making it unlikely that a similar structure could form (see Figure 1C). As a result, we predict that the SH3 domain in PLCG1 as well as that in SLAP2 could form a similarly kinked structure with extended N- and C-terminal contacts.

Wild-Type Extension of Domain C, Including the Proline Rich Binding Motif. In full-length CIN85, domain C is immediately followed by a stretch of four proline rich motifs named P1−P4 (Figure 1A). P1 is separated from the C-terminal residue, Glu333, of the longest construct of domain C (C35) by only four residues. There are several examples in the literature of SH3 domains adjacent to proline rich motifs, e.g., in tec and in the p85 subunit of PI3-kinase where an interaction is observed between the SH3 domain and the proline rich motifs, either in an intramolecular fashion as in tec kinase[37,38] or in an intermolecular fashion as in the case of the p85 subunit of PI-3 kinase.[39] In principle, such interactions could also exist for domain C of CIN85. Such an interaction should significantly increase the thermal stability of the SH3 domain. However, the melting temperature of construct C53 [containing domain C and P1, residues Asp263−Pro346 (see Figures 1A and 2A)] was only marginally improved over those of the other constructs of domain C (Figure 3). A molecular dynamics (MD) simulation confirmed that the linker is too short for an intramolecular interaction by showing dissociation within 3−5 ns of the MD trajectory in water (Figure S5 of the Supporting Information). This result was supported by NMR data that showed no significant chemical shift perturbations of the residues in the canonical binding site (Figure 8A), similar rotational correlation times τ_c for C35 (Asp263−Glu333, 5.8 ± 0.2 ns) and C53 (Asp263−Arg346, 6.2 ± 0.2 ns), low order parameters for the additional residues (Figure 8B), and analytical ultracentrifugation data that clearly show that construct C53 is a monomer (Figure 8C). To ensure that the extended construct C35 was still able to bind to proline rich motifs in principle, we studied the interaction with a Cbl-derived peptide, and the stoichiometry, affinity, and binding site were found to be in good agreement with values reported in the literature[40] (Figure S7 of the Supporting Information).

DISCUSSION

We initially started this work to produce optimized constructs of CIN85 SH3 domains in preparing for the study of larger fragments. Structure determination of CIN85 domain B has been successful[15] but was based on a construct that contained extra residues as a result of the cloning method (Figure 2A). Despite using the structure of domain B to guide the design of new constructs for domains B and C, we failed at first to obtain soluble protein. There are two NMR structures of domain B in the PDB, one determined by us (2O2O) and the other by the Riken structural genomics initiative (1WI7). Coincidentally, both of these contained a substantial number of extra random residues as a result of the cloning process (Figure 2A). Combined with the observations that there is no clear correlation between the length of the N- and C-terminal extension in our expression screen (Figure 3), this suggests that domain B will behave well as long as there are a few amino acids added at the N- and C-termini. These residues do not make any contact with the domain because the extensions of the two structures of domain B in the PDB are completely different from each other and also from the natural sequence of CIN85 that precedes and follows domain B (Figure 1B). Such a requirement for a number of residues might relate to the fact that this domain comes from a multidomain protein in which it is surrounded by long, polar, and flexible linkers. The complete absence of such sequence might render the SH3 domain difficult to fold or poorly soluble.

In contrast, the stabilization of domain C by N- and C-terminal extensions is based on a very well defined interaction not previously seen in SH3 domains. An extended C-terminus with a 90° bend while folding over the extended N-terminus has been observed in only one other SH3 domain.[36] However, while in this case contacts are made by backbone atoms leading to the formation of an antiparallel β-sheet, in CIN85 domain C the structure is more irregular and is dominated by salt bridges supported by hydrophobic interactions. The 1D spectra of the various extended constructs show that the hydrophobic interaction of Phe330 with Leu326 is not strong enough on its own (Figure 5). Instead, it requires the hydrophobic contact between Lys332 and Tyr271 and between the ultimate C-terminal Glu333 and its salt bridges and the N-terminal positively charged residues (Lys267 and Lys269) to achieve full cooperative stability. This is confirmed by the continuously increasing melting temperatures as the C-terminus is extended (Figure 4) and our molecular dynamics analysis (Figure 7)

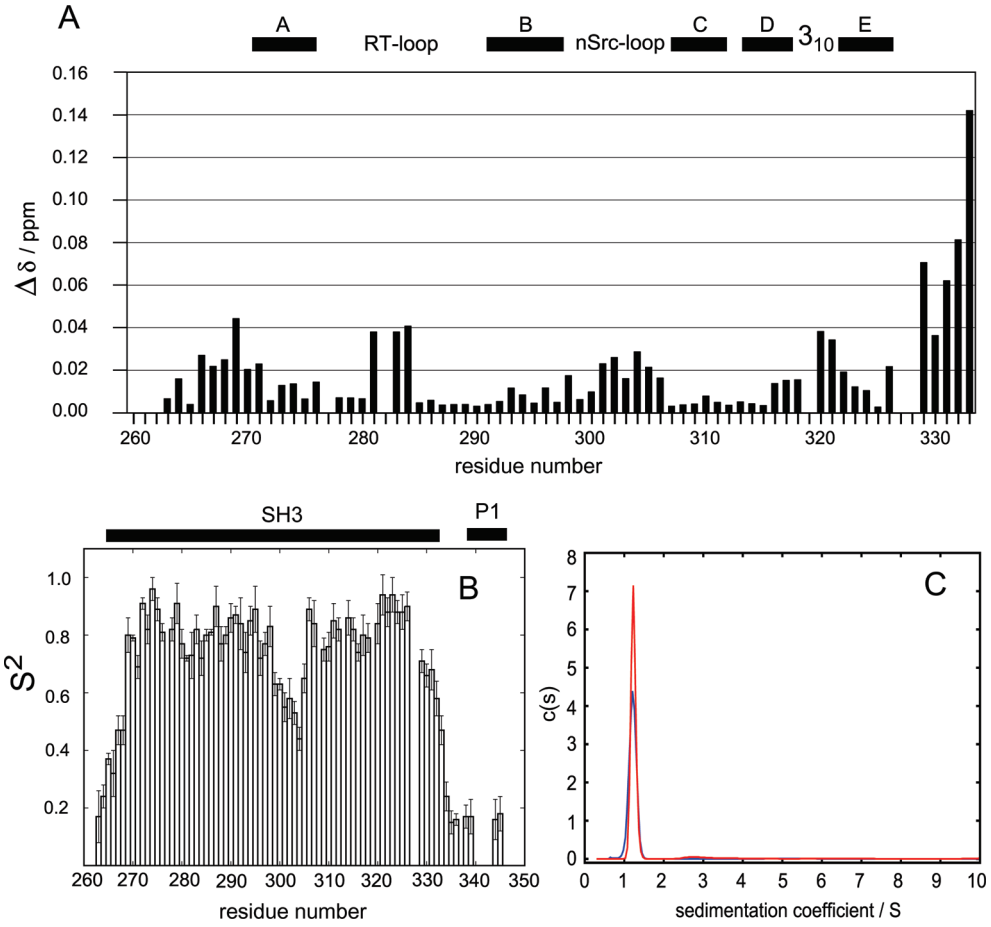

Figure 8. Effects of addition of the first proline rich motif (P1) that is located immediately C-terminal to domain C (domain C, construct C35, residues 263−333; P1, residues 337−346). (A) Plot of combined ^{1}H and ^{15}N chemical shift differences of construct C35 (domain C alone, residues 263−333) and construct C53 (domain C and the proximal proline rich motif P1, residues 263−346). (B) Results of the Lipari−Szabo analysis of ^{15}N relaxation data for construct C53. The positions of SH3 domain C and the proline rich motif P1 are indicated by bars above the graph. (C) Results of sedimentation velocity analytical ultracentrifugation of C35 (blue) and C53 (red).

The proline rich motifs immediately following the C-terminus (Figure 1) provide an opportunity for intra- or intermolecular interactions with domain C. An intramolecular interaction as in the case of tec kinase[37,38] is ruled out on the basis of the structure: the very extended C-terminus positions the proline rich motif too far from the canonical binding site, which puts significant strain on the linker, confirmed by a 10 ns molecular dynamics simulation showing that the intramolecular complex falls apart after ∼4 ns (Figure S5 of the Supporting Information). Preventing an intramolecular interaction of domain C with the following proline rich segment might indeed be the purpose of the C-terminal extension. The other option, an intermolecular interaction between domain C and its extended P1 linker, is theoretically possible just as in the case of, for example, PI3 kinase.[39] However, this option can easily be ruled out according to our extensive CD, NMR, and AUC investigations (Figure 8). Indeed, the addition of the full P1 motif only marginally increases the melting temperature (Figure 4) and does not alter the oligomerization state of the domain as evidenced by ^{15}N relaxation and analytical ultracentrifugation data. As a result, there is no interaction at all between domain C and the immediately following P1 segment. Control experiments were conducted to ensure that the extended version of the domain is capable of binding to proline rich ligands (Figure S6 of the Supporting Information).

In this work, we demonstrate comprehensively that the folding and potential function even of well-established protein domains can depend on residues well outside the canonical domain definition. The effect of N- and C-terminal extensions on domain C showed high sequence specificity reflected in the interactions observed in the NMR structure and confirmed by molecular dynamics simulations. Identifying the correct domain boundaries in this case preserves an unusual structural feature that otherwise would be missed. This structural feature is very likely required for the function of CIN85. It is quite clearly able to prevent an intramolecular interaction of domain C with its immediately following proline rich motif P1, which could be an important asset when full-length CIN85 forms a complex with targets such as Cbl or p85 proteins.

A very simple and conservative sequence analysis based on the key interactions for this novel structural extension of a SH3 domain identified two such domains in human proteins, SLAP2 and PLCG1, for which we predict a very similar, extended structure. It is too early to try to derive functional conclusions from this group of proteins; however, it is interesting to note that both SLAP2 and PLCG1 interact with various Cbl isoforms, and for PLCG1 and CIN85, it was shown that the SH3 domains are required for binding to Cbl.[41] These findings suggest that widening the scope of sequence analysis to allow for alternative

interactions of extended N- and C-termini allows even more SH3 domains with an extended structure to be found, and consequently, this novel structure could exist in more SH3 domains. This emphasizes the importance of terminal residues on the fringes for the overall stability, structure, and function of protein domains.

■ ASSOCIATED CONTENT

Supporting Information. Example melting curves of two constructs of domain C (Figure S1), more distances from a MD trajectory of construct C35 (Figure S2), a comparison of HSQC spectra of constructs C33 and C35 (Figure S3), an extended view of structural superpositions of the structure of domain C with related structures (Figure S4), distance traces and structure snapshots of a 10 ns MD trajectory of construct C53 to complement the experimental data in Figure 8 (Figure S5), interaction experiments to show that the extended construct of domain C (C35) is able to bind to proline rich peptides (Figure S6). This material is available free of charge via the Internet at http://pubs.acs.org.

■ AUTHOR INFORMATION

Corresponding Author

*Phone: 00442078486478. Fax: 00442078486435. E-mail: mark.pfuhl@kcl.ac.uk.

Present Addresses

[@]Cardiovascular and Randall Division, King's College London, Guy's Campus, London SE1 1UL, U.K.

Funding Sources

This work was funded by a BBSRC grant to M.P. and J.E.L. (BB/D018994/1).

■ ACKNOWLEDGMENT

We thank Dr. F. Muskett for help with NMR spectrometers and Dr. K. Sidhu for help with computers.

■ ABBREVIATIONS

ITC, isothermal titration calorimetry; NMR, nuclear magnetic resonance; RDC, residual dipolar couplings; CD, circular dichroism; NOESY, nuclear Overhauser enhancement spectroscopy; MD, molecular dynamics; SH3 domain, src homology domain 3; IPTG, isopropyl thiogalactoside.

■ REFERENCES

(1) Go, M. (1985)Protein Structures and Split Genes. *Adv. Biophys. 19*, 91–131.

(2) Holland, S. K., and Blake, C. C. (1987)Proteins, Exons and Molecular Evolution. *BioSystems 20*, 181–206.

(3) Liu, M., and Grigoriev, A. (2004)Protein Domains Correlate Strongly with Exons in Multiple Eukaryotic Genomes: Evidence of Exon Shuffling?. *Trends Genet. 20*, 399–403.

(4) Basu, M. K., Poliakov, E., and Rogozin, I. B. (2009)Domain Mobility in Proteins: Functional and Evolutionary Implications. *Brief Bioinf. 10*, 205–216.

(5) Kirillova, S., Kumar, S., and Carugo, O. (2009)Protein Domain Boundary Predictions: A Structural Biology Perspective. *Open Biochem. J. 3*, 1–8.

(6) Castiglione Morelli, M. A., Stier, G., Gibson, T., Joseph, C., Musco, G., Pastore, A., and Trave, G. (1995)The KH Module has an $\alpha\beta$ Fold. *FEBS Lett. 358*, 193–198.

(7) Pfuhl, M., Improta, S., Politou, A. S., and Pastore, A. (1997) When a Module is also a Domain: The Importance of the N-Terminus in the Dynamics and the Stability of Immunoglobulin Domains from Titin. *J. Mol. Biol. 265*, 242–256.

(8) Take, H., Watanabe, S., Takeda, K., Yu, Z. X., Iwata, N., and Kajigaya, S. (2000)Cloning and Characterization of a Novel Adaptor Protein, CIN85, that Interacts with c-Cbl. *Biochem. Biophys. Res. Commun. 268*, 321–328.

(9) Kowanetz, K., Husnjak, K., Holler, D., Kowanetz, M., Soubeyran, P., Hirsch, D., Schmidt, M. H., Pavelic, K., De Camilli, P., Randazzo, P. A., and Dikic, I. (2004)CIN85 Associates with Multiple Effectors Controlling Intracellular Trafficking of Epidermal Growth Factor Receptors. *Mol. Biol. Cell 15*, 3155–3166.

(10) Holler, D., and Dikic, I. (2004)Receptor Endocytosis Via Ubiquitin-Dependent and Indepentent Pathways. *Biochem. Pharmacol. 67*, 1013–1017.

(11) Jozic, D., Cardens, N., Deribe, Y. L., Moncalian, G., Hoeller, D., Groemping, Y., Dikic, I., Rittinger, K., and Bravo, J. (2005)Cbl Promotes Clustering of Endocytic Adaptor Proteins. *Nat. Struct. Biol. 12*, 972–979.

(12) Gout, I., Middleton, G., Adu, J., Ninkina, N. N., Drobot, L. B., Filokenko, V., Matsuka, G., Davies, A. M., Waterfield, M., and Buchman, V. L. (2000)Negative Regulation of PI 3-Kinase by Ruk, a Novel Adaptor Protein. *EMBO J. 19*, 4015–4025.

(13) Borthwick, E. B., Korobko, I. V., Luke, C., Drel, V. R., Fedyshyn, Y. Y., Drobot, L. B., and Buchman, V. L. (2004)Multiple Domains of Ruk/CIN85/SETA/CD2BP3 are Involved in Interaction with p85a Regulatory Subunit of PI 3-Kinase. *J. Mol. Biol. 343*, 1135–1146.

(14) Ababou, A., Pfuhl, M., and Ladbury, J. E. (2008)The Binding Stoichiometry of CIN85 SH3 Domain A and Cbl-b. *Nat. Struct. Mol. Biol. 15*, 890–891.

(15) Ababou, A., Pfuhl, M., and Ladbury, J. E. (2009)Novel Insights into the Mechanisms of CIN85 SH3 Domains Binding to Cbl Proteins: Solution-Based Investigations and in Vivo Implications. *J. Mol. Biol. 387*, 1120–1136.

(16) Sigrist, C. J., Cerutti, L., de Castro, E., Langendijk-Genevaux, P. S., Bulliard, V., Bairoch, A., and Hulo, N. (2010)PROSITE, a Protein Domain Database for Functional Characterization and Annotation. *Nucleic Acids Res. 38*, D161–D166.

(17) Thompson, J. D., Higgins, D. G., and Gibson, T. J. (1994) Clustal W: Improving the Sensitivity of Progressive Multiple Sequence Alignment through Sequence Weighting, Position-Specific Gap Penalties and Weight Matrix Choice. *Nucleic Acids Res. 22*, 4673–4680.

(18) Larkin, M. A., Blackshields, G., Brown, N. P., Chenna, R., McGettigan, P. A., McWilliam, H., Valentin, F., Wallace, I. M., Wilm, A., Lopez, R., Thompson, J. D., Gibson, T. J., and Higgins, D. G. (2007) Clustal W and Clustal X Version 2.0. *Bioinformatics 23*, 2947–2948.

(19) Marley, J., Lu, M., and Bracken, C. (2001)A Method for the Efficient Isotopic Labeling of Recombinant Proteins. *J. Biomol. NMR 20*, 71–75.

(20) Kay, L. E., Ikura, M., Tschudin, R., and Bax, A. (1990)Three-Dimensional Triple Resonance NMR Spectroscopy of Isotopically Enriched Proteins. *J. Magn. Reson. 89*, 496.

(21) Vranken, W. F., Boucher, W., Stevens, T. J., Fogh, R. H., Pajon, A., Llinas, M., Ulrich, E. L., Markley, J. L., Ionides, J., and Laue, E. D. (2005)The CCPN Data Model for NMR Spectroscopy: Development of a Software Pipeline. *Proteins 59*, 687–696.

(22) Lipari, G., and Szabo, A. (1982)Model-free approach to the interpretation of nuclear magnetic resonance relaxation in macromolecules. 1. Theory and range of validity. *J. Am. Chem. Soc. 104*, 4546–4559.

(23) Lipari, G., and Szabo, A. (1982)Model-free approach to the interpretation of nuclear magnetic resonance relaxation in macromolecules. 2. Analysis of experimental results. *J. Am. Chem. Soc. 104*, 4559–4570.

(24) Kay, L. E., Nicholson, L. K., Delaglio, F., Bax, A., and Torchia, D. A. (1992)Pulse Sequences for Removal of the Effects of Cross

Correlation between Dipolar and Chemical Shift Anisotropy Relaxation Mechanism on the Measurement of Heteronuclear T_1 and T_2 Values in Proteins. *J. Magn. Reson. 97*, 359–367.

(25) Barbato, G., Ikura, M., Kay, L. E., Pastor, R. W., and Bax, A. (1992)Backbone Dynamics of Calmodulin Studied by ^{15}N Relaxation using Inverse Detected Two-Dimensional NMR Spectroscopy: The Central Helix is Flexible. *Biochemistry 31*, 5269–5278.

(26) Güntert, P., and Wüthrich, K. (1991)Improved Efficiency of Protein Structure Calculations from NMR Data using the Program DIANA with Redundant Dihedral Angle Constraints. *J. Biomol. NMR 1*, 447–456.

(27) Cornilescu, G., Delaglio, F., and Bax, A. (1999)Protein Backbone Angle Restraints from Searching a Database for Chemical Shift and Sequence Homology. *J. Biomol. NMR 13*, 289–302.

(28) Brunger, A. T. (1993) *XPLOR*, version 3.1, Yale University, New Haven, CT.

(29) Holm, L., and Sander, C. (1993)Protein Structure Comparison by Alignment of Distance Matrices. *J. Mol. Biol. 233*, 123–138.

(30) Holm, L., and Sander, C. (1995)Dali: A Network Tool for Protein Structure Comparison. *Trends Biochem. Sci. 20*, 478–480.

(31) Case, D. A., Darden, T., Cheatham, T. E., III, Simmerling, C. L., Wang, J., Duke, R. E., Luo, R., Merz, K. M., Wang, B., Pearlman, D. A., Crowley, M., Brozel, S., Tsui, V., Gohlke, H., Mongan, J., Hornak, V., Cui, G., Beroza, P., Schafmeister, C., Caldwell, J. E., Ross, W. S., and Kollman, P. A. (2004) *Amber 8*, University of California, San Francisco.

(32) Schuck, P. (2000)Size-Distribution Analysis of Macromolecules by Sedimentation Velocity Ultracentrifugation and Lamm Equation Modeling. *Biophys. J. 78*, 1606–1619.

(33) Laue, T. M., Shah, B. D., Ridgeway, T. M., and Pelletier, S. L. (1992) Computer-Aided Interpretation of Analytical Sedimentation Data for Proteins. In *Ultracentrifugation in Biochemistry and Polymer Science* (Harding, S. E., Rowe, A. J., and Horton, J. C., Eds.) pp 90−125, Royal Society of Chemistry, Cambridge, U.K.

(34) Haun, R. S., Serventi, I. M., and Moss, J. (1992)Rapid, Reliable Ligation-Independent Cloning of PCR Products using Modified Plasmid Vectors. *BioTechniques 13*, 515–518.

(35) Bezsonova, I., Bruce, M. C., Wiesner, S., Lin, H., Rotin, D., and Forman-Kay, J. D. (2008)Interactions between the Three CIN85 SH3 Domains and Ubiquitin: Implications for CIN85 Ubiquitination. *Biochemistry 47*, 8937–8949.

(36) Wisniewska, M., Bossenmaier, B., Georges, G., Hesse, F., Dangl, M., Kunkele, K. P., Ioannidis, I., Huber, R., and Engh, R. A. (2005)The 1.1 Å Resolution Crystal Structure of the p130cas SH3 Domain and Ramifications for Ligand Selectivity. *J. Mol. Biol. 347*, 1005–1014.

(37) Brazin, K. N., Fulton, D. B., and Andreotti, A. H. (2000)A Specific Intermolecular Association between the Regulatory Domains of a Tec Family Kinase. *J. Mol. Biol. 302*, 607–623.

(38) Pursglove, S. E., Mulhern, T. D., Mackay, J. P., Hinds, M. G., and Booker, G. W. (2002)The Solution Structure and Intramolecular Associations of the Tec Kinase SRC Homology 3 Domain. *J. Biol. Chem. 277*, 755–762.

(39) Harpur, A. G., Layton, M. J., Das, P., Bottomley, M. J., Panayotou, G., Driscoll, P. C., and Waterfield, M. D. (1999)Intermolecular Interactions of the p85α Subunit of Phosphstidylinositol 3-Kinase. *J. Biol. Chem. 274*, 12323–12332.

(40) Kowanetz, K., Szymkiewicz, I., Haglund, K., Kowanetz, M., Husnjak, K., Taylor, J. D., Soubeyran, P., Engstrom, U., Ladbury, J. E., and Dikic, I. (2003)Identification of a Novel Proline-Arginine Motif Involved in CIN85-Dependent Clustering of Cbl and Down-Regulation of Epidermal Growth Factor Receptors. *J. Biol. Chem. 278*, 39735–39746.

(41) Tvorogov, D., and Carpenter, G. (2002)EGF-Dependent Association of Phospholipase C-γ1 with c-Cbl. *Exp. Cell Res. 277*, 86–94.